

Document downloaded from:

<http://hdl.handle.net/10251/39895>

This paper must be cited as:

Reig Cerdá, L.; Amigó Borrás, V.; Busquets Mataix, DJ.; Calero Martinez, JA. (2012). Development of porous Ti6Al4V samples by microsphere sintering. *Journal of Materials Processing Technology*. 212(1):3-7. doi:10.1016/j.jmatprotec.2011.06.026.



The final publication is available at

<http://dx.doi.org/10.1016/j.jmatprotec.2011.06.026>

Copyright Elsevier

## Accepted Manuscript

Title: Development Of Porous Ti6al4 v Samples By  
Microsphere Sintering

Authors: Lucía Reig, Vicente Amigó, David J. Busquets, Jose  
A. Calero



PII: S0924-0136(11)00196-8  
DOI: doi:10.1016/j.jmatprotec.2011.06.026  
Reference: PROTEC 13183

To appear in: *Journal of Materials Processing Technology*

Received date: 20-5-2011  
Revised date: 27-6-2011  
Accepted date: 29-6-2011

Please cite this article as: Reig, L., Amigó, V., Busquets, D.J., Calero, J.A., Development Of Porous Ti6al4 v Samples By Microsphere Sintering, *Journal of Materials Processing Technology* (2010), doi:10.1016/j.jmatprotec.2011.06.026

This is a PDF file of an unedited manuscript that has been accepted for publication. As a service to our customers we are providing this early version of the manuscript. The manuscript will undergo copyediting, typesetting, and review of the resulting proof before it is published in its final form. Please note that during the production process errors may be discovered which could affect the content, and all legal disclaimers that apply to the journal pertain.

**DEVELOPMENT OF POROUS Ti6Al4V SAMPLES BY MICROSPHERE SINTERING**

LUCÍA REIG<sup>a</sup>, VICENTE AMIGÓ<sup>b</sup>, DAVID J. BUSQUETS<sup>b</sup>, JOSE A. CALERO<sup>c</sup>

<sup>a</sup> Department of Mechanical Engineering and Construction, Universitat Jaume I, Avda. de Vicent Sos Baynat, s/n, 12071 Castelló de la Plana, Spain

<sup>b</sup> Mechanical and Materials Engineering Department, Polytechnic University of Valencia, Camino de Vera s/n, 46022 Valencia, Spain

<sup>c</sup> Aleaciones de Metales Sinterizados S.A. (AMES), San Vicenç dels Horts, Barcelona, Spain

---

Corresponding author: L. Reig; Tel.: +34 964 729163, Fax: +34 964 728106  
E-mail address: [lreig@emc.uji.es](mailto:lreig@emc.uji.es); [vamigo@mcm.upv.es](mailto:vamigo@mcm.upv.es); [dbusquets@mcm.upv.es](mailto:dbusquets@mcm.upv.es);  
[jacalero@ames.es](mailto:jacalero@ames.es);

## ABSTRACT

Two differently sized microspheres were sintered at 1300 °C and 1400 °C from 2 to 8 hours in stoneware, alumina, yttria and zirconia moulds. Selecting the appropriate material to be used as a mould remains a critical issue given titanium's high reactivity at elevated temperatures. Optimum mechanical properties were obtained when sintering the smallest microspheres in yttria-coated moulds. Stiffness of the samples was lower than 40% of that of the bulk solid material, which comes closer to that of human cortical bone. Open and interconnected porosity was observed in all the specimens.

Keywords: Porous titanium; microsphere sintering; bending strength; stiffness; metallic implant.

## 1. Introduction

Despite titanium having been widely used in biomedical applications, its stiffness is excessive when compared to that of human cortical bone (10-40 GPa) (Asaoka, 2003). According to Ryan et al. (2006), this can cause weakening and may lead to the implant coming loose. This problem can be mitigated in a variety of ways. Several authors, such as Kuroda (2005) and Niinomi (2008), have reduced the stiffness of this material by increasing the amount of  $\beta$ -type alloying elements, which has led to the development of alloys such as Ti30Ta, Ti35Nb7Zr5Ta or Ti30Nb, with a Young's Modulus of only 58, 55 and 42 GPa, respectively. Stiffness can also be reduced by developing a porous network. According to Degischer and Kriszt (2002), solid phase techniques have proved more suitable than liquid phase foaming methods due to titanium's high melting point and high reactivity. As reported by Amigó et al. (2003), microsphere sintering is a solid phase technique that has been widely used to produce titanium coatings in order to facilitate bone in-growth. Nevertheless, it has never been used to develop completely porous parts. A critical issue when producing samples following this procedure is the machining process because beads tend to come off the sample when they are subjected to cutting or grinding, especially as the microsphere size increases. For this reason, and in order to analyse the influence of the material used as a mould on the mechanical properties obtained, samples were tested without machining. This also made it possible to determine whether machining could be avoided after sintering by selecting the appropriate mould material.

This paper aimed to analyse the influence of microsphere size, sintering temperature and time, together with the material used as a mould, on the mechanical properties of porous specimens developed by sintering Ti6Al4V microspheres.

## 2. Experimental Procedure

### 2.1. Raw material

Spherical Ti6Al4V alloy beads were supplied by Phelly Materials Inc. These were manufactured by the plasma rotating electrode process (PREP), previously described by Wosche et al. (1995). The chemical composition shown in Table I is in agreement with specification ASTM F1580-01 for Ti6Al4V powders used for surgical and medical implant coatings.

Table I. Chemical composition of Ti6Al4V beads made by the PREP process

Elements	Al	V	O	Fe	C	H	N	Cu	Sn	Ti
ASTM F1580-01	5.5-6.75	3.5-4.5	0.2	0.3	0.08	0.015	0.05	0.1	0.1	Balance
Ti64, GF	6.45	4.15	0.12	0.13	0.041	0.004	0.029	<0.05	<0.05	Balance
Ti64, GG	6.15	4.18	0.076	0.072	0.016	0.002	0.006	<0.01	<0.01	Balance

As shown in Figure 1, two particle sizes were selected in this study, referenced as “fine” (FG) and “coarse” (CG). Apparent and tap densities were determined according to standard ASTM B213-97, using an AcuPowder Hall International flowmeter. As expected (German, 2005), apparent density was lower for fine microspheres (FG: 2.64 g/cm<sup>3</sup>; CG: 2.82 g/cm<sup>3</sup>). The value increased to around 2.82 g/cm<sup>3</sup> after applying slight vibration, which is of vital importance when developing a higher neck area between neighbouring microspheres during the sintering process.

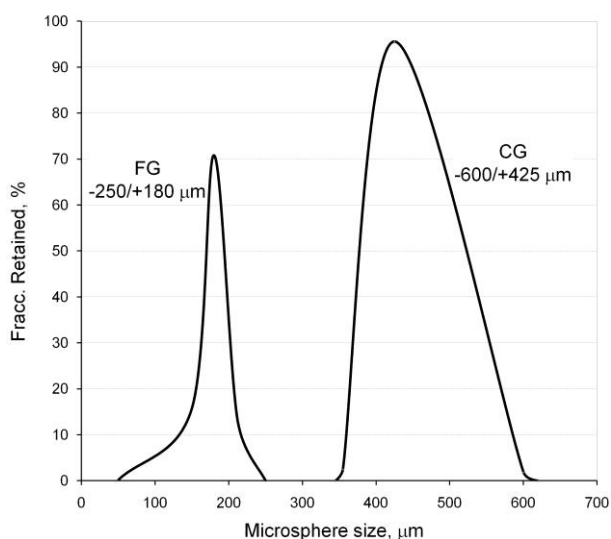


Figure 1. Size distribution of Ti6Al4V microspheres produced by the PREP process

The raw material was characterised by optical and electron microscopy using a Nikon Microphot FX and a JEOL JSM6300 Scanning Electron microscope, respectively, the latter also being equipped with an EDX detector model 6508 (Oxford Instruments Ltd). Figure 2 shows the fine Widmstätten microstructure of the raw material, composed of thin layers of alternating  $\alpha$  and  $\beta$ , which, according to Leyens and Peters (2003), results from a high cooling rate while manufacturing by the PREP process.

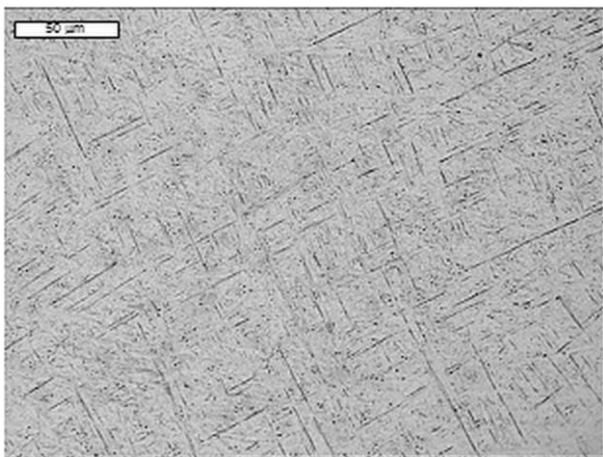


Figure 2. Microstructure of the coarse Ti6Al4V beads produced by the PREP process. Etching: Kroll reagent

## 2.2. Development of porous Ti6Al4V specimens by microsphere sintering

Stoneware, alumina, yttria and zirconia were used as mould materials. Stoneware was selected because it is easy to shape, while the rest of the ceramic materials were chosen for their stability. Ti6Al4V beads were poured into the mould under gravity. Slight vibration was applied to increase the number of contact points between microspheres. Sintering was performed in an HVT 15/75/450 Carbolite vacuum furnace ( $10^{-4}$ - $10^{-5}$  mBar). Sintering temperatures and times were chosen in accordance with previous studies, such as those conducted by Amigó et al. (2011) and Reig et al. (2011), in which porous titanium specimens were produced following the space-holder method. Samples were sintered between 1300 °C and 1400 °C from 2 to 8 hours. Table II summarises the procedure followed and the process variables.

Table II. Process variables used in the development of porous Ti6Al4V by sintering beads

Sintering temperatures, °C	1300, 1350, 1400
Sintering times, h	2, 4, 8
Microsphere sizes	FG: -250/+180 $\mu\text{m}$ ; CG: -425/+600 $\mu\text{m}$
Materials used as moulds	Stoneware, $\text{Al}_2\text{O}_3$ , $\text{Y}_2\text{O}_3$ , $\text{Zr}_2\text{O}_3$

Stoneware moulds were produced in the laboratory by mixing clay with ceramic particles (>4 mm) in order to minimise shrinkage, drying and firing. Alumina and zirconia moulds were supplied by Keratec Advanced Materials SA. Yttria (99.9%) powder, supplied by CymitQuimica SL, was used to coat the alumina moulds. This coating was replaced after each sintering cycle.

### 2.3. Characterisation of porous specimens

The microstructure of the samples was observed by means of optical and scanning electron microscopy. Apparent density ( $\rho^*$ ), porosity and pore size were determined by PIM using an AutoPore IV (9500). A bulk density ( $\rho_s$ ) of 4.42 g/cm<sup>3</sup> (ASM, 1990) was used to calculate the relative density of the samples ( $\rho_r = \rho^*/\rho_s$ ). Microhardness was measured by applying a load of 25 g for 15 s in a Matsuzawa HT2 microhardness tester.

Bending strength was determined by a three-point bending test in accordance with ASTM E290-97a (ISO 3325:2000) specifications in an Instron 4204 at a crosshead speed of 0.5 mm/min. For this purpose, rectangular specimens with a width of 10-12 mm were used. Due to mould restrictions, thickness ( $e$ ) varied from  $e \approx 4.5$ -5.5 mm for the stoneware and  $e \approx 3.3$ -4.5 mm for the zirconia, alumina and yttria moulds. Tests were performed under the most unfavourable conditions, i.e. placing the side in contact with the mould while sintering under tensile stress. Stiffness was determined by the ratio between maximum deflection by bending and load (1):

$$E = \left( \frac{F \cdot l^3}{4 \cdot y_{\max} \cdot b \cdot e^3} \right) \quad (1)$$

where  $E$  = stiffness (MPa),  $F$  = Force (N),  $l$  = distance between supports (19.5 mm),  $y_{\max}$  = maximum deflection (mm),  $b$  and  $e$  = width and thickness (mm) of the specimen.

To obtain the relative stiffness of the porous Ti6Al4V parts ( $E_r = E/E_s$ ), the stiffness of a sample produced by conventional powder metallurgy techniques was used as a reference, which was



called bulk solid stiffness,  $E_s$ . As explained by Reig et al. (2011), for this purpose Ti6Al4V powder, produced by hydration-dehydration, was pressed at 300 MPa and sintered at 1300 °C for 2h.

### 3. Results

The porosity of the sintered samples was open and interconnected, was only slightly affected by the sintering parameters and was around 32% for both microsphere sizes. The mean pore size diameter was 55 (30-80) and 140 (70-190)  $\mu\text{m}$  for the porous samples developed using the FG and CG microspheres, respectively. As Figure 3 shows, the raw material's microstructure was modified during the sintering process. Grain coarsening was observed for those samples sintered at higher temperatures or for longer times.

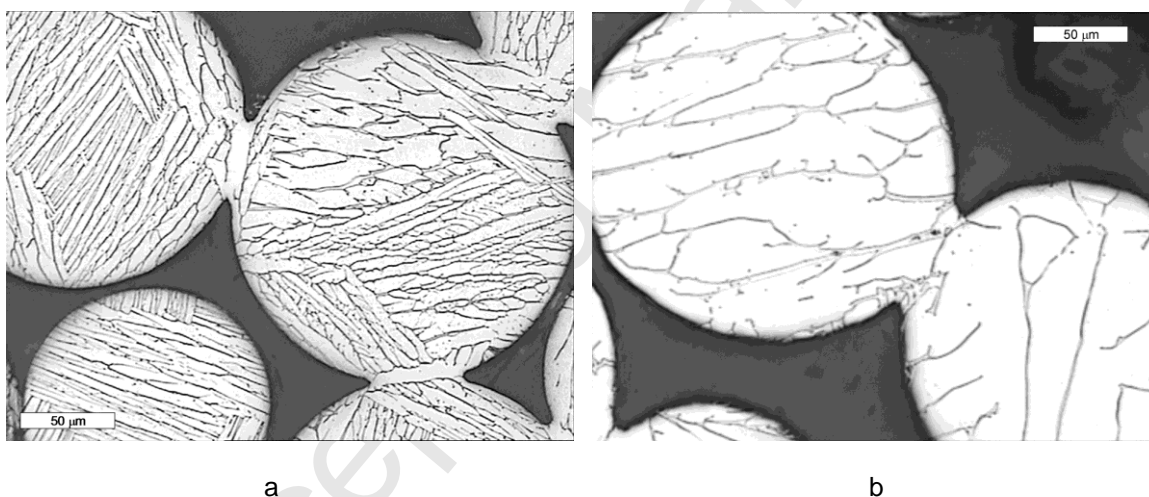


Figure 3. Microstructure of the smaller Ti6Al4V microspheres after sintering in yttria moulds: a) 1300 °C, 2h; b) 1400 °C, 8h. Etching: Kroll reagent

The spherical shape and chemical composition of those microspheres sintered in stoneware and alumina moulds was modified during the sintering process (see Figure 4). When using stoneware, the microspheres in contact with the mould partially melted, and typical clay components like Si, Na were found after the EDX analysis. When alumina was used as the mould material, the microspheres in contact with the mould cracked and the aluminium content increased significantly. Cracks were only observed when sintering was performed in alumina.

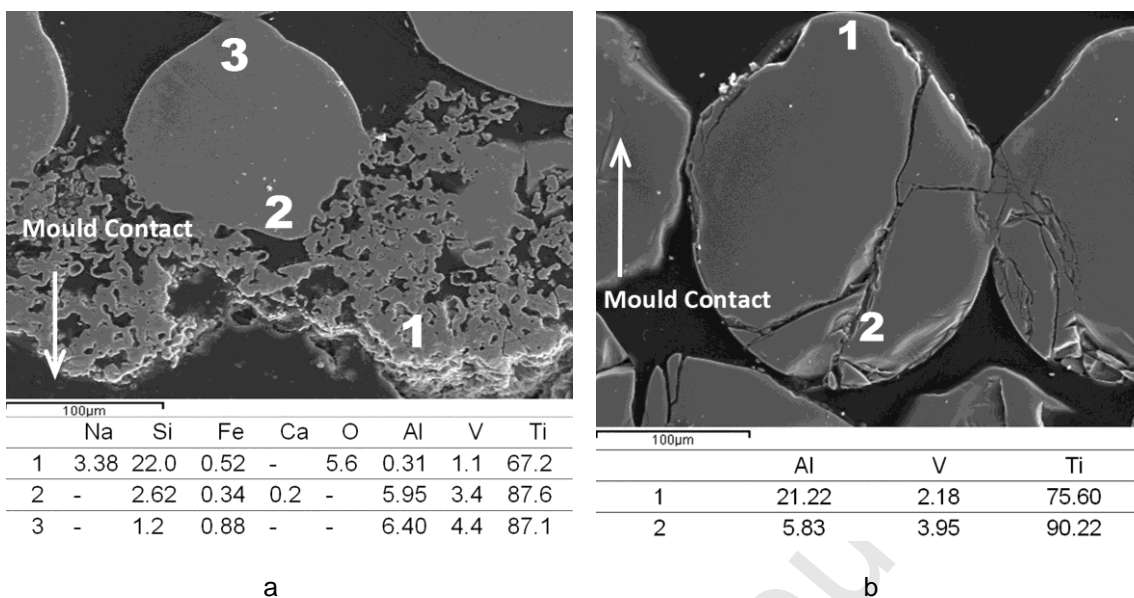


Figure 4. SEM micrograph and EDX analyses (% wt) of the Ti6Al4V beads sintered in: a) Stoneware; b) Alumina

Reactivity with zirconia moulds was found to depend mainly on sintering temperature and time, and was completely deleterious in terms of mechanical strength. As sintering temperatures increased, a change in the morphology of the microspheres in contact with the mould was observed (see Figure 5a), thus illustrating a completely brittle cleavage fracture after the bending test (see Figure 5b).

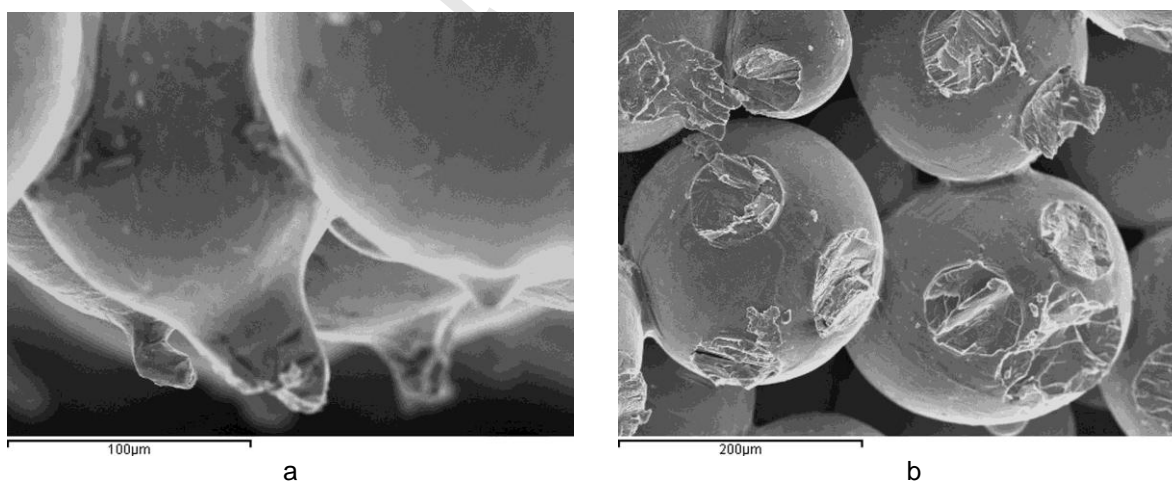


Figure 5. SEM micrograph of the Ti6Al4V beads sintered in zirconium oxide at 1400 °C for 8 hours: a) Mould contact area; b) Bending test fracture area

The specimens sintered in yttria retained their shape during sintering, but revealed ductile fracture characteristics at the microlevel (see Figure 6a). Despite reactivity being minimal when yttria was used as the mould material, elements diffused through the coating and reacted with the alumina of the substrate at higher temperatures or longer sintering cycles, especially at 1400 °C for 8h (see Figure 6b).

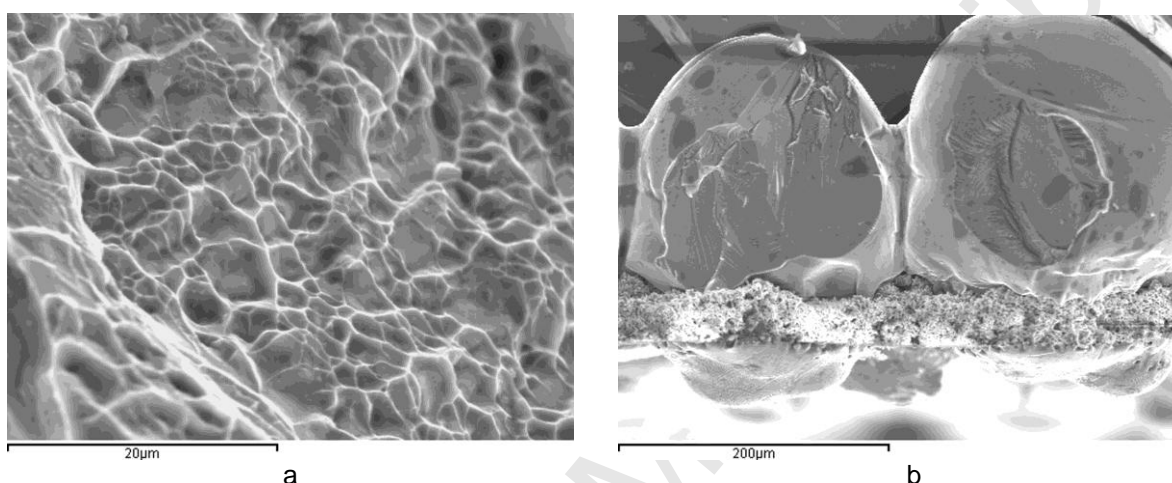


Figure 6. SEM micrograph of the Ti6Al4V beads sintered in yttria at 1400 °C for 8 hours: a) Ductile fracture; b) Reactivity with the underlying alumina mould

Influence of the mould was confirmed by microhardness analyses (see Figure 7). Softening was observed when sintering only in yttria, which, as previously reported by Felton et al. (2009), is due to the absence of reactivity and the grain coarsening originated by slow cooling rates, which are attained under vacuum conditions. Maximum hardness was found for those beads sintered in alumina.

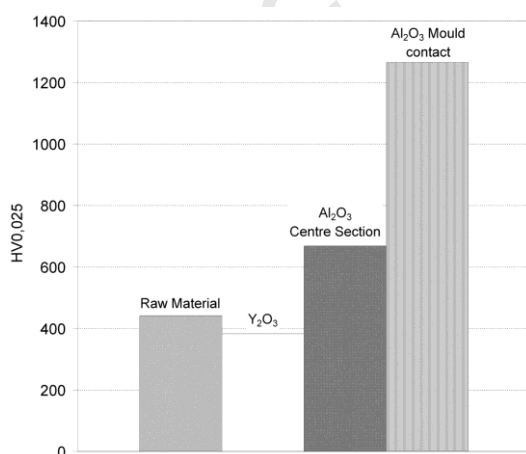


Figure 7. Microhardness of Ti6Al4V beads before and after sintering in Al<sub>2</sub>O<sub>3</sub> and Y<sub>2</sub>O<sub>3</sub> at 1350 °C for 8 hours

As shown in Table III, the best mechanical properties were obtained when sintering in yttria. A direct correlation between bending strength and sintering temperature and time was only observed when this material was used as the support for the microspheres. Stiffness of the samples was less than 40% of that obtained for the bulk solid material.

Table III. Bending strength and relative stiffness of the porous specimens developed

T, °C	t, h	ME size	Yttria		Stoneware	Alumina	Zirconia
			$\sigma_{YF}$ , MPa	Er	$\sigma_{YF}$ , MPa	$\sigma_{YF}$ , MPa	$\sigma_{YF}$ , MPa
1300	2	FG	131	0.25			68
		CG	41	0.13			31
	4	FG	169	0.25		83	87
		CG	53	0.12		32	43
	8	FG	239	0.40	54	68	107
		CG	73	0.12	22	32	59
1350	2	FG	145	0.30		84	76
		CG	37	0.10		34	35
	4	FG	162	0.27		61	109
		CG	48	0.17		27	45
	8	FG	288	0.34		63	105
		CG	77	0.23		24	58
1400	2	FG	192	0.31	76	40	106
		CG	52	0.18	30	21	42
	4	FG	241	0.43	66		149
		CG	74	0.18	24		70
	8	FG	320	0.53	93		
		CG	106	0.26	28		

Figure 8 shows the mechanical properties of the porous samples sintered in yttria. As depicted by the fitting curve proposed, bending strength increases linearly with sintering temperature (T, °C), logarithmically with sintering time (t, h), and decreases for those raw microspheres with larger diameters ( $d_i$ ,  $\mu\text{m}$ ). Maximum deviation from the proposed curves was noted for the smaller microspheres sintered at 1350 °C and 1400 °C for 8 hours, due to some reactivity with the alumina substrate through the yttria coating.

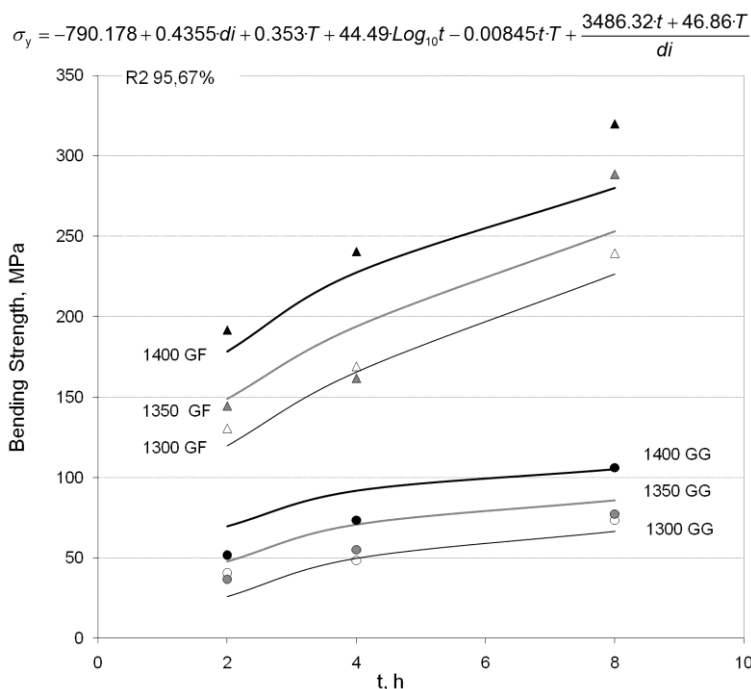


Figure 8. The bending strength and correlation model of the porous Ti6Al4V specimens sintered in yttria

#### 4. Discussion

In microspheres that come into contact with stoneware moulds,  $\text{Ti}_x\text{Si}_y$  intermetallics are formed at sintering temperatures of 1300-1400 °C. As illustrated in the Si-Ti phase diagram (ASM, 1997), they transformed while cooling, thereby giving rise to eutectic and peritectic compounds. Similarly, intermetallic compounds ( $\text{Ti}_3\text{Al}$ ,  $\text{TiAl}$ ) were formed when sintering in alumina moulds, which are responsible for embrittling these microspheres. These results are in agreement with the thermodynamic analysis reported by Kostov et al. (2006), who concluded that alumina, when in contact with Ti6Al4V, is more unstable than expected given its energy of formation ( $\Delta G^{\circ}_f$ ). Despite zirconium oxide having been used as a substrate to develop titanium specimens (Esteban, 2008), it is not suitable for developing porous Ti6Al4V samples by microsphere sintering because, according to the Ellingham diagram (Muñoz, 2005), this ceramic loses stability at approximately 1220 °C when it comes into contact with titanium oxides. As yttria is the most stable ceramic, net-shaped yttria moulds could be used to avoid the undesirable reaction between the titanium microspheres and the underlying alumina. The problem is that such moulds are difficult to produce.

According to Asaoka and Kon (2003), the reduced stiffness achieved will diminish bone re-absorption problems. Furthermore, the bending strength of human cortical bone ( $\approx 100$  MPa) (Heimann, 2002) can only be accomplished when sintering smaller microspheres. Nevertheless, the possibility of bone in-growth is much stronger when porous samples are developed by sintering coarser beads because, according to several authors such as Bansiddhi et al. (2008) and Bram et al. (2005), a minimum pore size from 100 to 500 microns is required to generate bone cells and blood vessels, respectively. However, some bone in-growth can also be expected in porous specimens made by sintering smaller microspheres, since Kujala et al. (2003) demonstrated bone in-growth with smaller pore sizes (50 to 125 microns) when no load is applied.

## 5. Conclusions

Porous Ti6Al4V samples have been developed by microsphere sintering. The mould material used has proved to be a critical issue because machining the obtained specimens is a very complex process. A bending strength that is high enough to allow these samples to be used as a bone substitute can be obtained only when sintering in yttria. The stiffness of these samples comes closer to that of human cortical bone. The samples presented herein have an open and interconnected porosity with pore sizes ranging from 30 to 190 microns.

## Acknowledgements

The authors are grateful to the Spanish Ministry of Science and Innovation for supporting this study through Project PET2008\_0158\_02.

The translation of this paper was funded by the Polytechnic University of Valencia and the Universitat Jaume I.

## References

- Amigó, V., Salvador, M.D., Romero, F., Solves, C., Moreno, J.F., 2003. Microstructural evolution of Ti-6Al-4V during the sintering of microspheres of Ti for orthopedic implants. *J. Mater. Process. Tech.*, 141, 117-122.
- Amigó, V., Reig, L., Busquets, D. J., Ortiz, J. L., Calero, J.A., 2011. Analysis of bending strength of porous titanium processed by space holder method. *Powder Metall.*, DOI: 10.1179/174329009X409697.
- Asaoka, K., Kon, M., 2003. Sintered porous titanium and titanium alloys as advanced biomaterials. *Thermec'2003*, PTS 1-5 426-4, 3079-3084.
- ASM International, 1990. *ASM Handbook Vol.2: Heat treating*, p. 1170.
- ASM International, 1997. *ASM Handbook Vol.3: Alloy Phase Diagrams*, pp. 54-367.
- Bansiddhi, A., Sargeant, T.D., Stupp, S.I., Dunand, D.C., 2008. Porous NiTi for bone implants: A review. *Acta Biomater.* 4, 773-782.
- Bram, M., Bogdanski, S.H., Koller, M., Buchkremer, H.P., Stover, D., 2005. Evaluation of Mechanical and Biological properties of highly porous Titanium parts. *Euro PM2005. PM Applications*, 517-522.
- Degischer, H.P., Kriszt B., 2002. *Handbook of Cellular Metals: Production, Processing, Applications: Wiley-VCH*, pp. 22-184.
- Esen, Z., Bor, S., 2007. Processing of titanium foams using magnesium spacer particles. *Scripta Materialia*, 56 (5), 341-344.
- Esteban, P. G., Ruiz-Navas, E. M., Bolzoni, L., Gordo, E., 2008. Low-cost titanium alloys? Iron may hold the answers. *Metal Powder Report* 63 (4), 24-27.
- Felton, R., Imgrund, P.H., Petzoldt, F., Friederici, V., Busquets-Mataix, D, Reig, L., Amigó, V., Calero, J.A., 2009. PM companies eye a new future of taking medicine. *Metal Powder Report* 64, 12-17.
- German, R.M., 2005. *Powder metallurgy and particulate materials processing: the processes, materials, products, properties and applications*, Ed. Metal Powder Industries Federation.
- Gil, F.J., 2007. Comparison of the mechanical properties between tantalum and nickel-titanium foams implant materials for bone ingrowth applications. *J. Alloy. Compd.*, 439 (1-2), 67-73.
- Heimann, R.B., 2002. *Materials Science of Crystalline Bioceramics: A Review of Basic Properties and Applications*. *CMU Journal* 1, 23-46.
- Kostov, A., Friedrich, B., 2006. Predicting thermodynamic stability of crucible oxides in molten titanium and titanium alloys. *Comput. Mater. Sci.* 38, 374-385.

- Kujala, S., Ryhanen, J., Danilov, A., Tuukkanen, J., 2003. Effect of porosity on the osteointegration and bone ingrowth of a weight-bearing nickel-titanium bone graft substitute. *Biomaterials*, 24 (25), 4691-4697.
- Kuroda, D., Kawasaki, H., Yamamoto, A., Hiromoto, S., Hanawa, T., 2005. Mechanical properties and microstructures of new Ti-Fe-Ta and Ti-Fe-Ta-Zr system alloys. *Mat. Sci. Eng.* 25 (3), 312 – 320.
- Leyens, C., Peters, M., 2003. *Titanium and Titanium Alloys. Fundamentals and Applications*, Ed. Wiley Vch Gmbh & Co, p. 423.
- Muñoz, M.J., 2005. *Principios de obtención de materiales*, Ed. UPV, p. 130.
- Niinomi, M., 2008. Mechanical biocompatibilities of titanium alloys for biomedical applications. *J. Mech. Behav. Biomed* 1 (1), 30-42.
- Reig, L., Amigó, V., Busquets, D., Calero, J.A., 2011. Stiffness variation of porous titanium developed using space holder method. *Powder Metall.*, DOI: 10.1179/003258910X12707304455068.
- Ryan, G., Pandit, A., Apatsidis, D.P., 2006. Fabrication methods of porous metals for use in orthopaedic applications. *Biomaterials* 27, 2651-2670.
- Wosche, E., Feldhaus, S., Gamm, T., 1995. Rapid solidification of steel droplets in the Plasma-Rotating-Electrode-Process. *ISIJ International*, 35 (6), 76477.



## LIST OF FIGURES:

Figure 1. Size distribution of Ti6Al4V microspheres produced by the PREP process

Figure 2. Microstructure of coarse Ti6Al4V beads produced by the PREP process. Etching: Kroll reagent

Figure 3. Microstructure of the smaller Ti6Al4V microspheres after sintering in yttria moulds: a) 1300 °C, 2h; b) 1400 °C, 8h. Etching: Kroll reagent

Figure 4. SEM micrograph and EDX analyses (% wt) of the Ti6Al4V beads sintered in: a) Stoneware; b) Alumina

Figure 5. SEM micrograph of the Ti6Al4V beads sintered in zirconium oxide at 1400°C for 8 hours: a) Mould contact area; b) Bending test fracture area

Figure 6. SEM micrograph of the Ti6Al4V beads sintered in yttria at 1400 °C for 8 hours: a) Ductile fracture; b) Reactivity with the underlying alumina mould

Figure 7. Microhardness of Ti6Al4V beads before and after sintering in Al<sub>2</sub>O<sub>3</sub> and Y<sub>2</sub>O<sub>3</sub> at 1350 °C for 8 hours

Figure 8. Bending strength and fitting curve of the porous Ti6Al4V specimens sintered in yttria

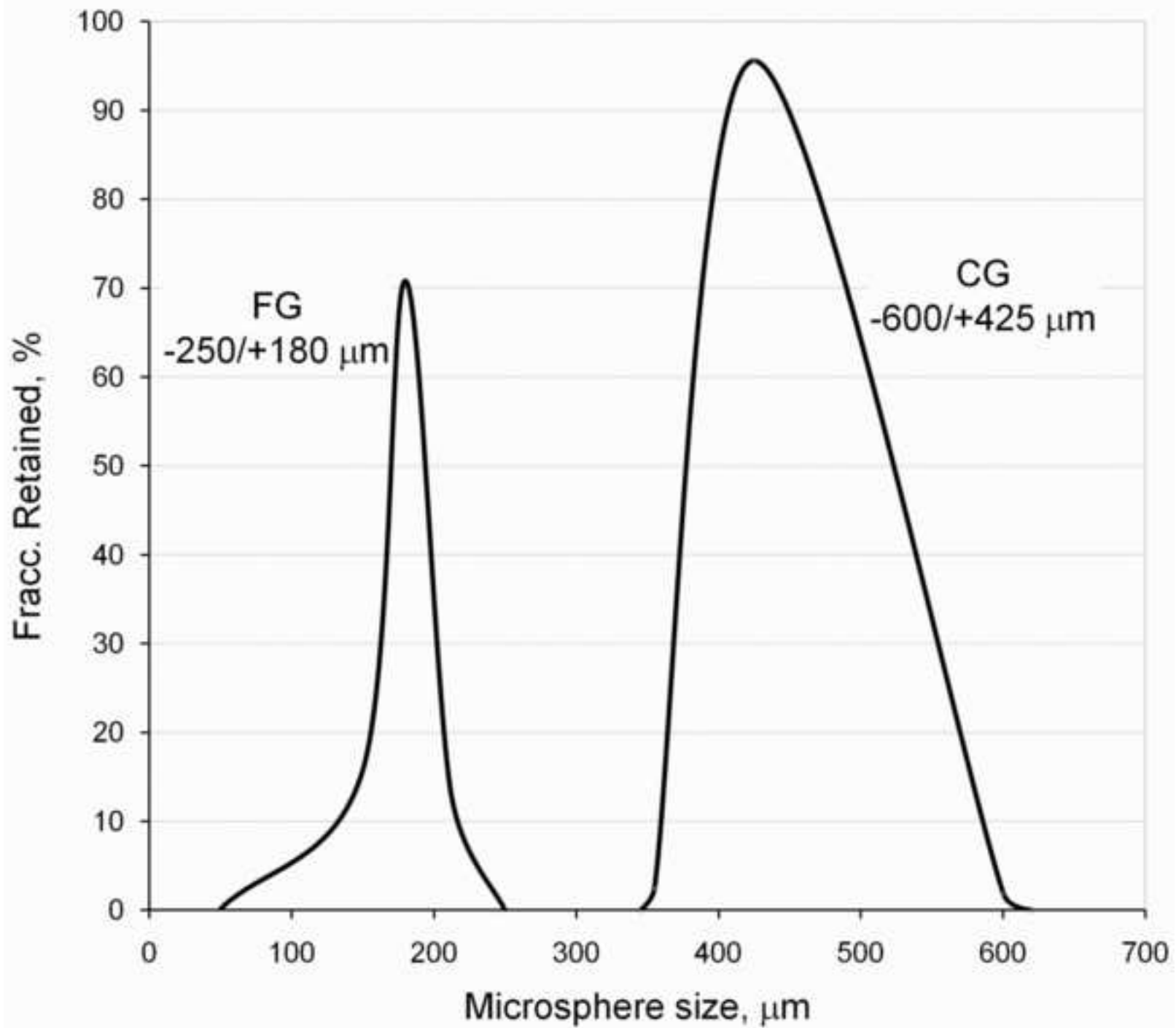
## LIST OF TABLES:

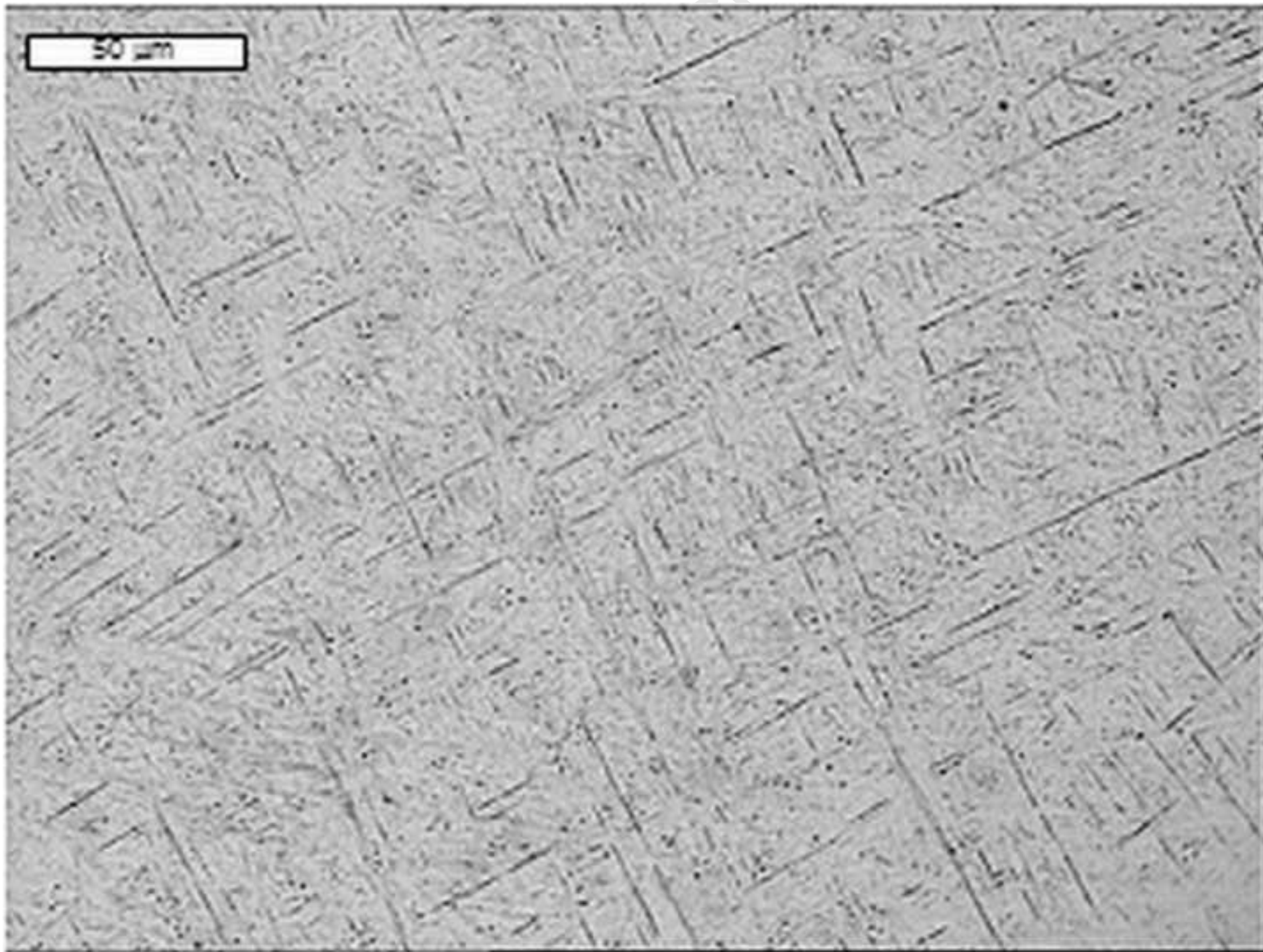
Table I. Chemical composition of Ti6Al4V beads produced by the PREP process

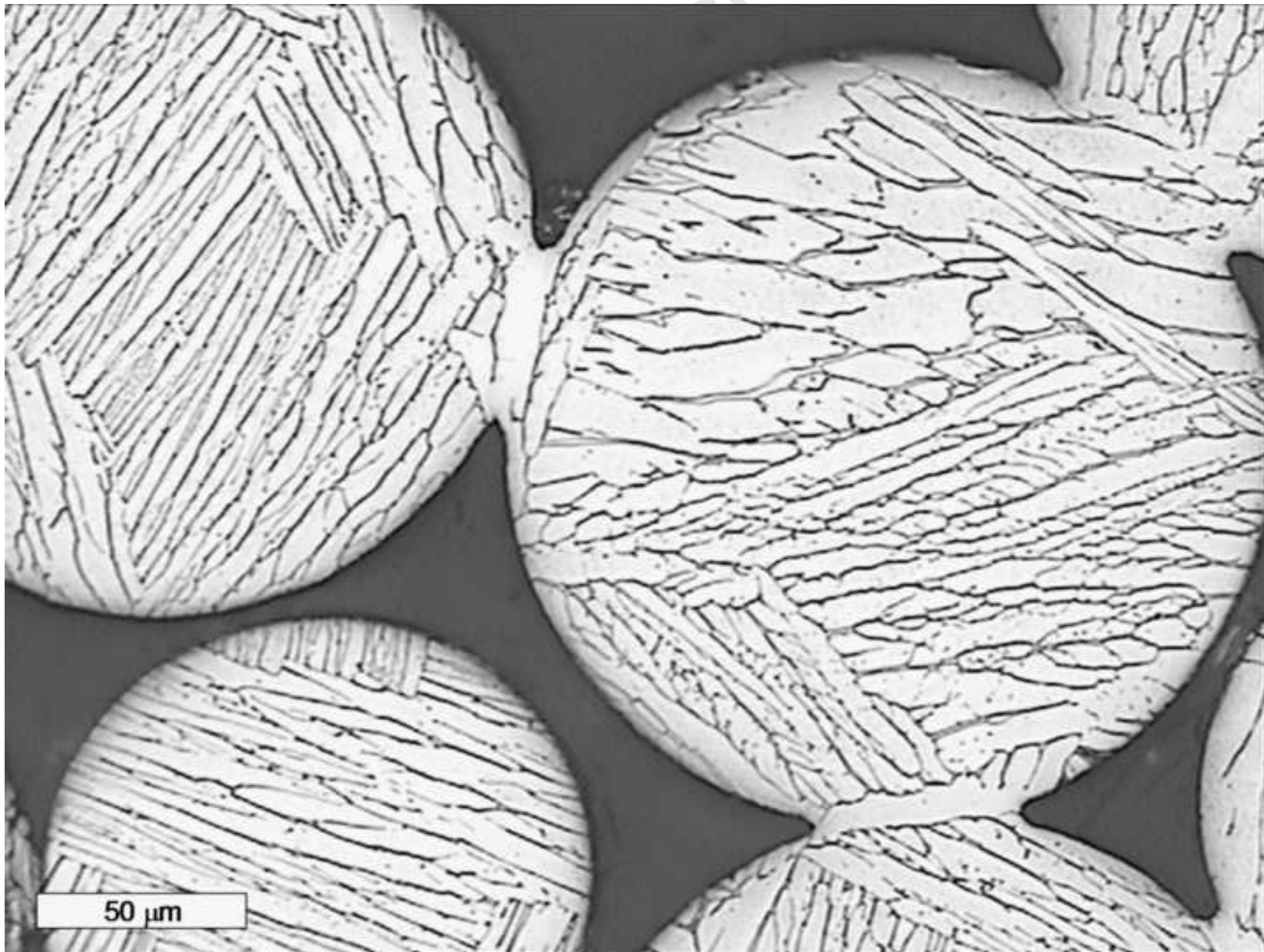
Table II. Process variables used in the development of porous Ti6Al4V by sintering beads

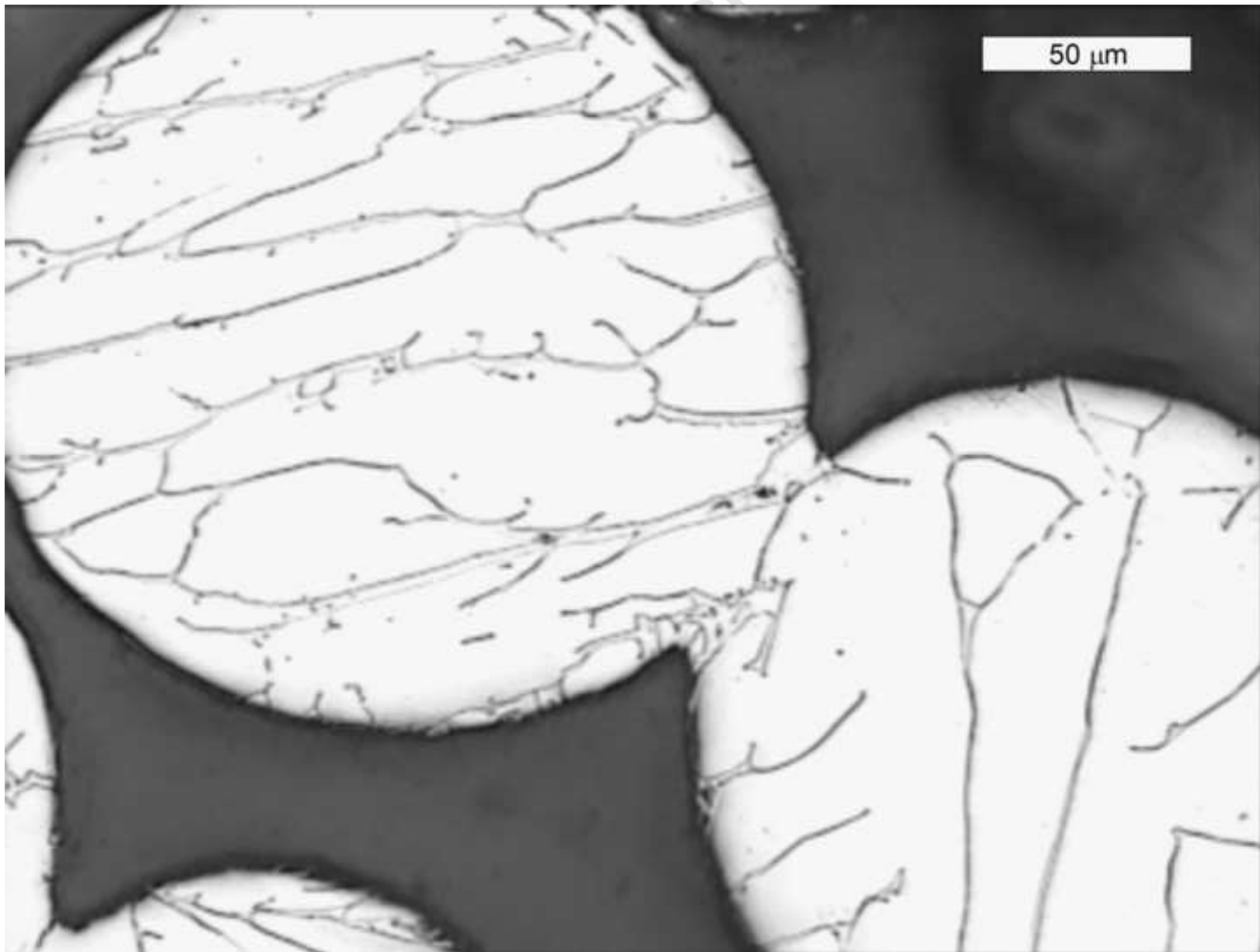
Table III. Bending strength and relative stiffness of the porous specimens developed

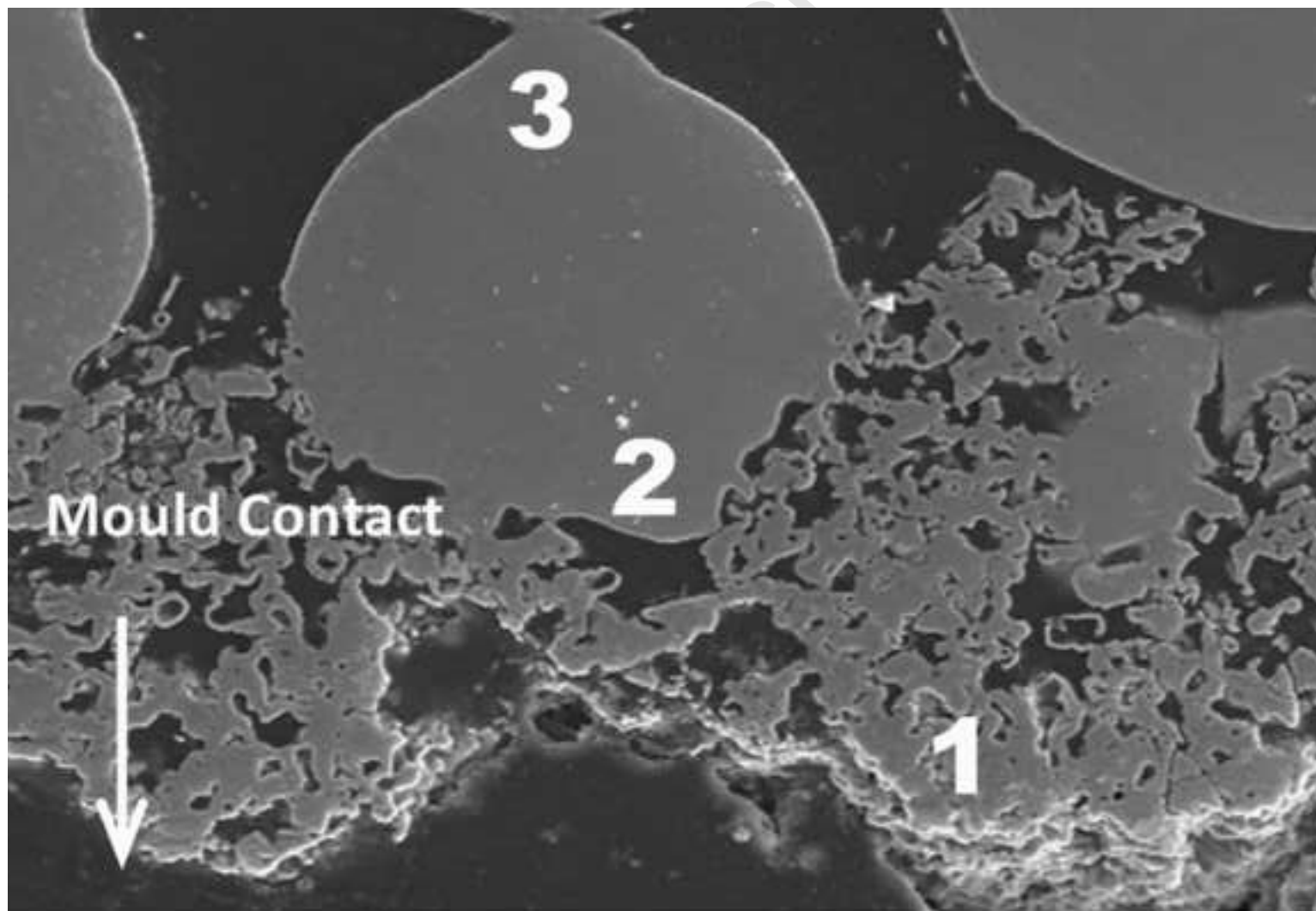
Accepted Manuscript



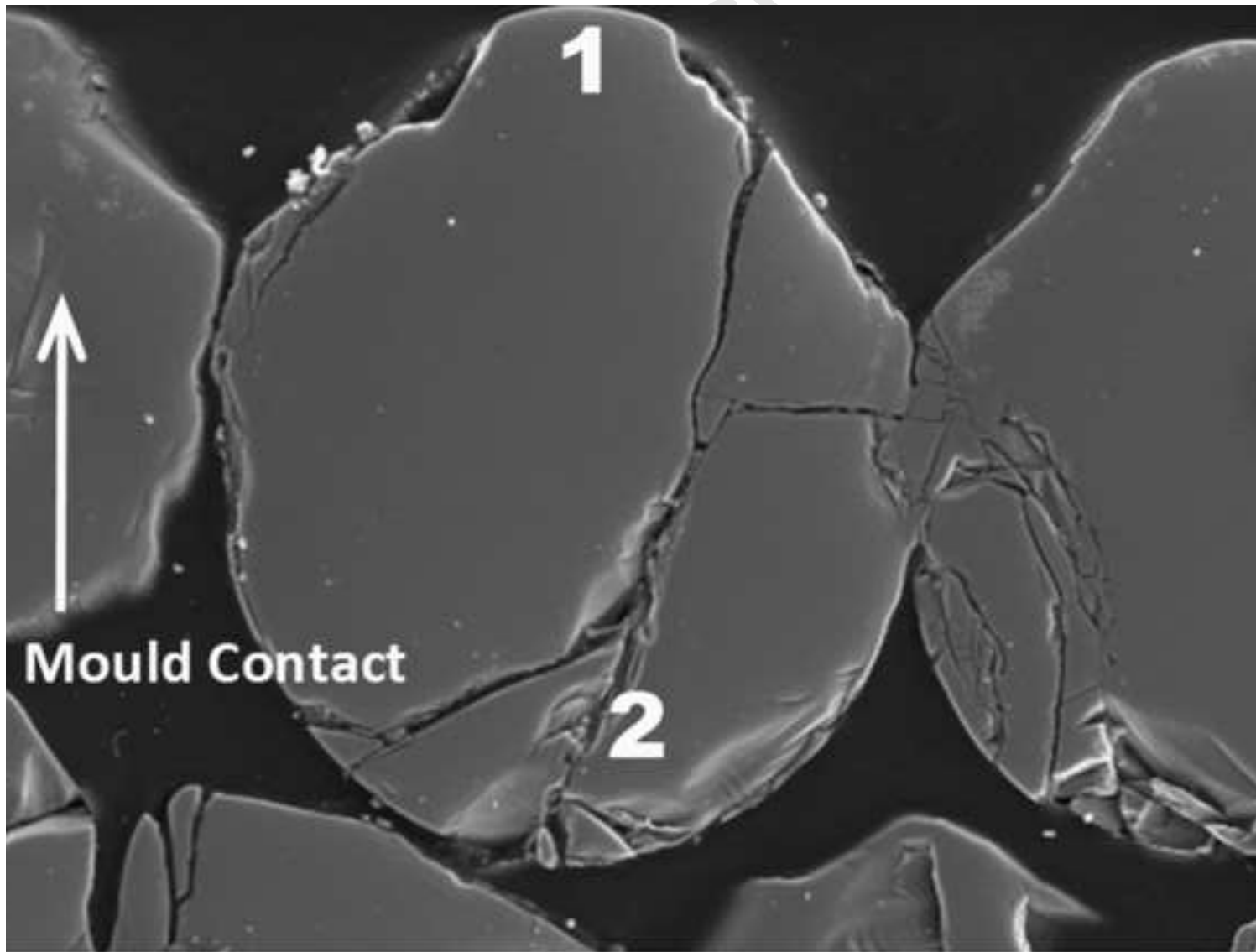






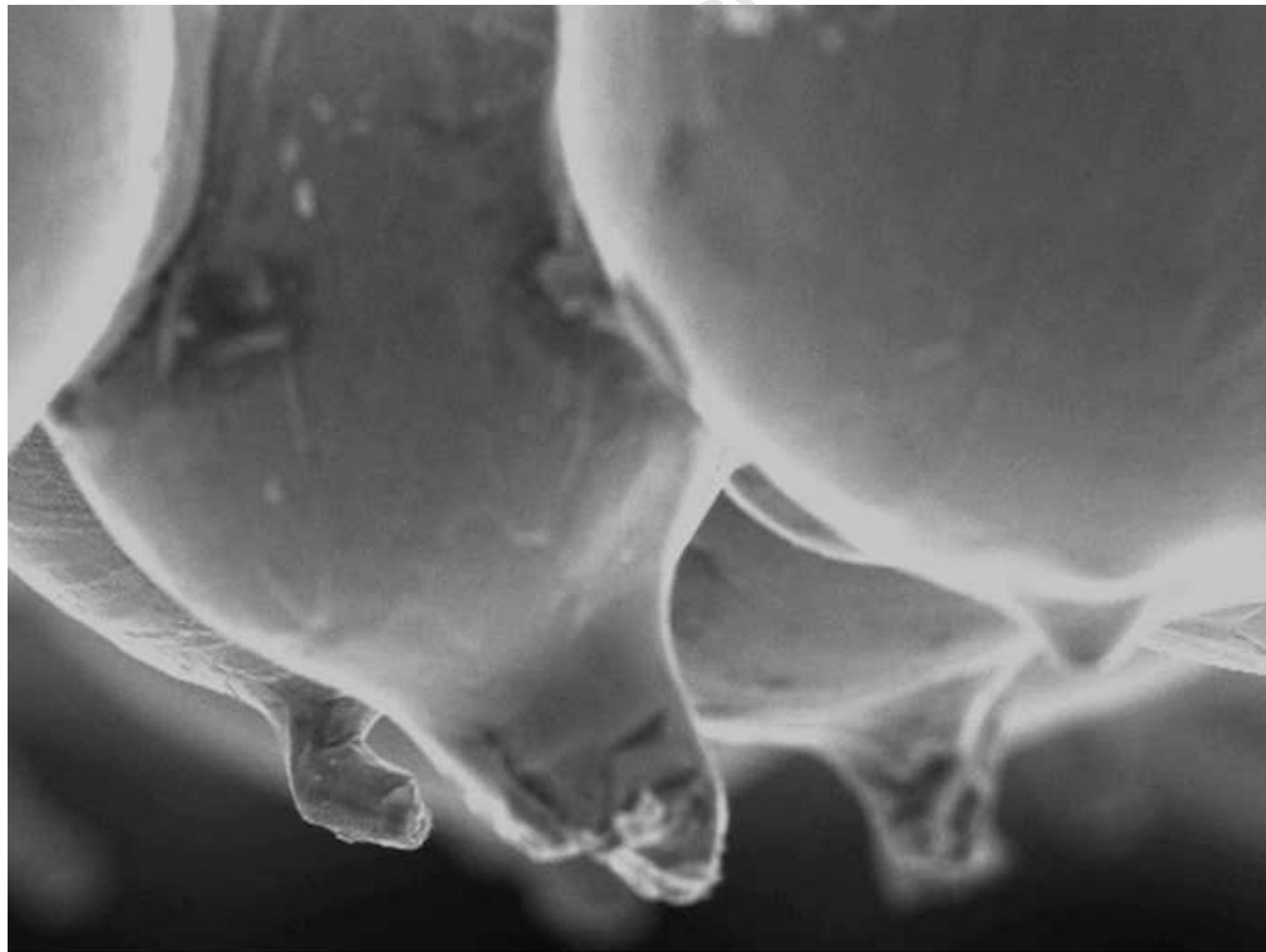


	Na	Si	Fe	Ca	O	Al	V	Ti
1	3.38	22.0	0.52	-	5.6	0.31	1.1	67.2
2	-	2.62	0.34	0.2	-	5.95	3.4	87.6
3	-	1.2	0.88	-	-	6.40	4.4	87.1

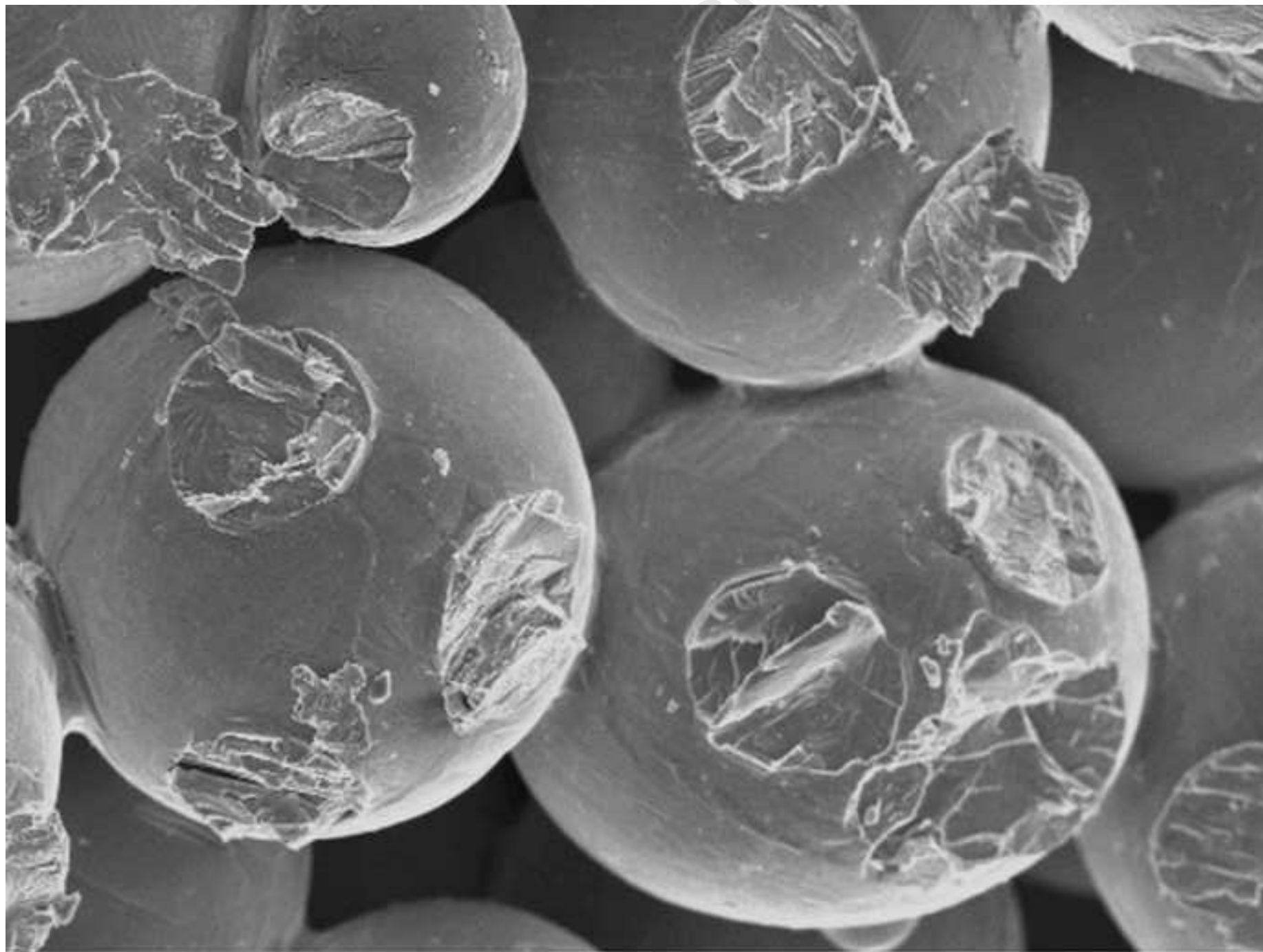


	Al	V	Ti
1	21.22	2.18	75.60
2	5.83	3.95	90.22

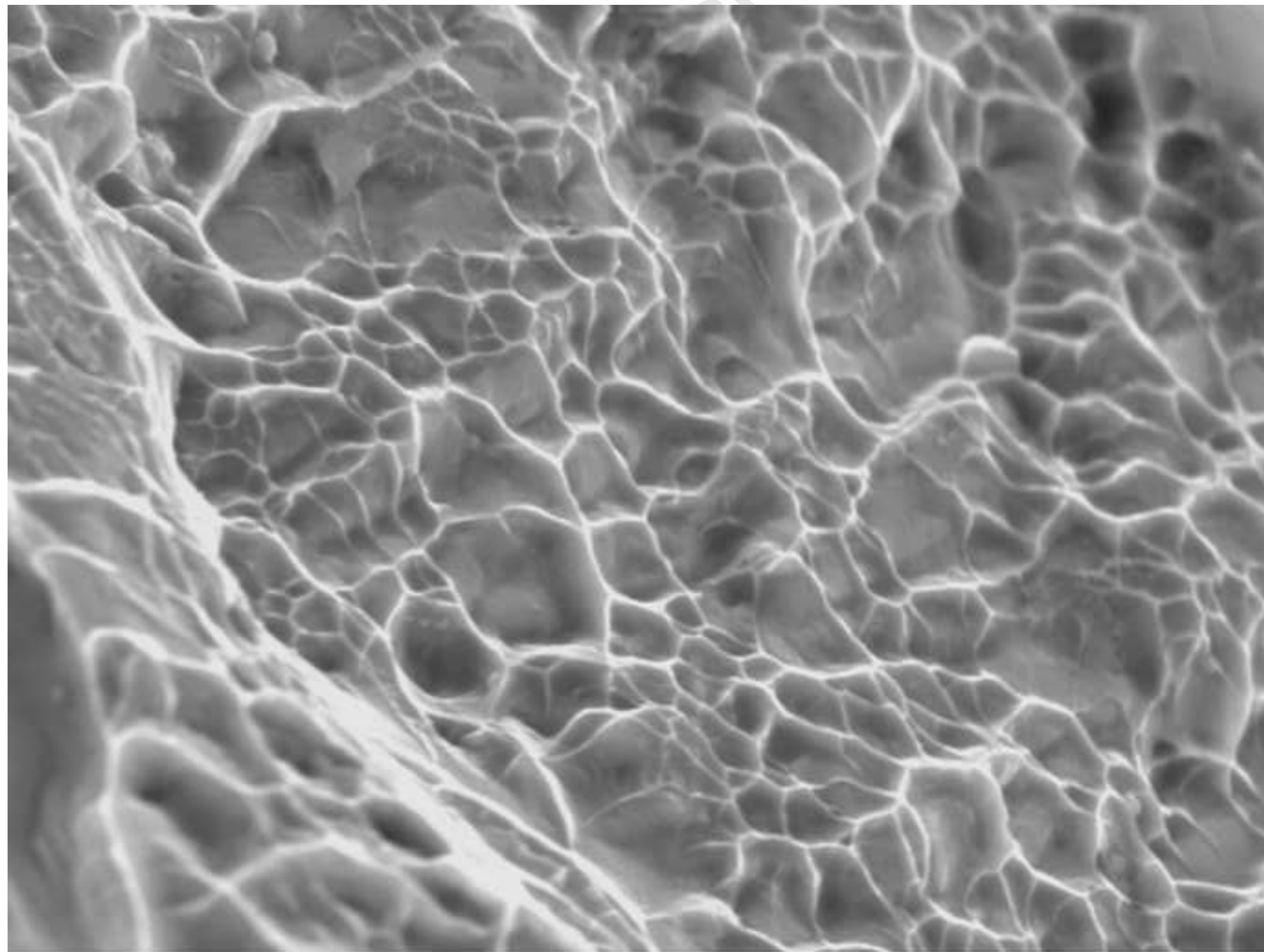




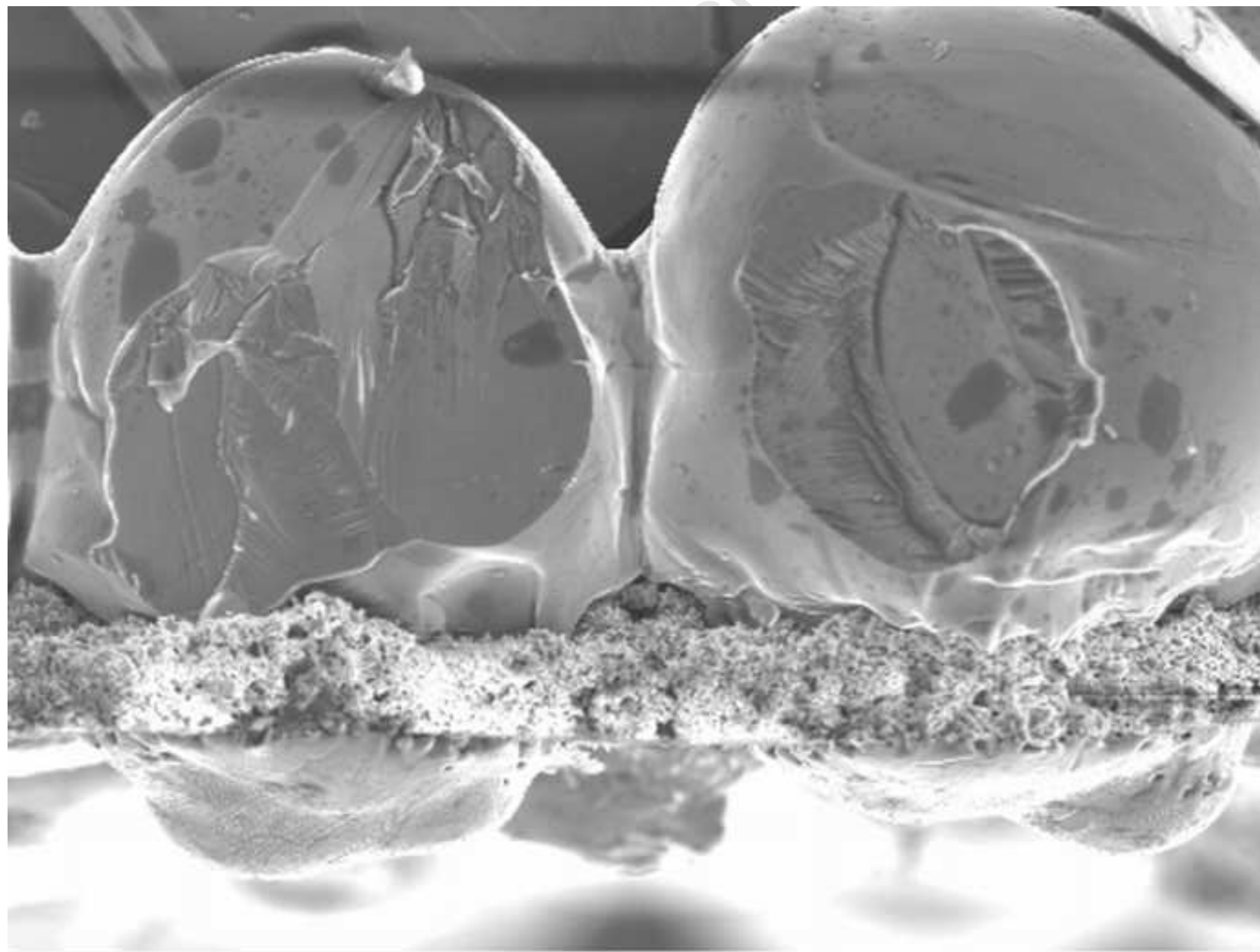
100µm



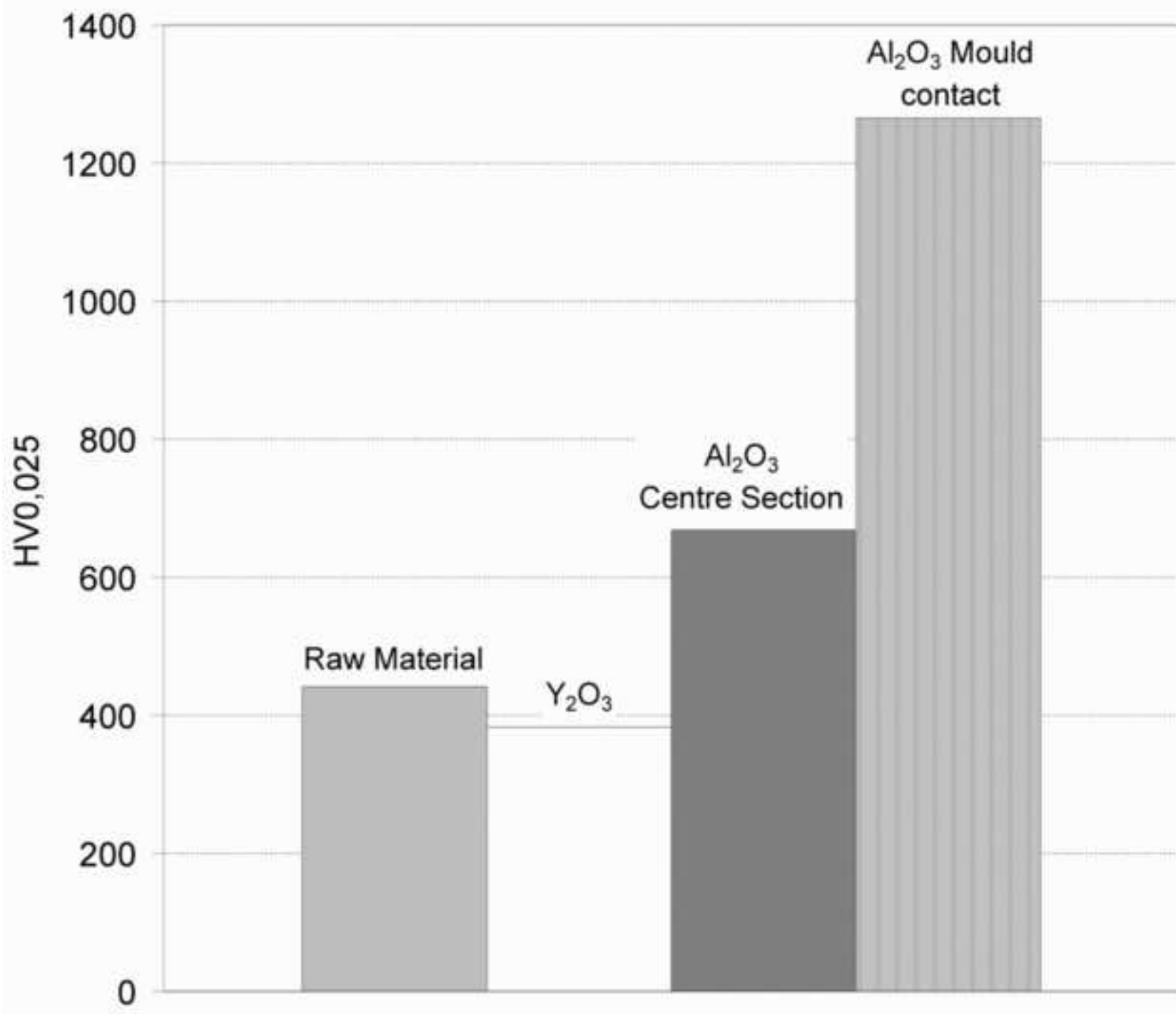
200 $\mu$ m



20 $\mu$ m



200µm



$$\sigma_y = -790.178 + 0.4355 \cdot di + 0.353 \cdot T + 44.49 \cdot \text{Log}_{10} t - 0.00845 \cdot t \cdot T + \frac{3486.32t + 46.86 \cdot T}{di}$$

